

EXPERIMENTAL AND NUMERICAL STUDY OF THE ISOMETRIC COGGED BIAXIAL GEOGRID (ICB-GGR)

Islam A. Elkorashi^{1*}, M. B. El Sideek¹, A. R. Hassan, Yousry Mowafy,
and Ahmed Farouk²

¹Department of Civil Engineering, Al-Azhar University, Cairo, Egypt.

²Assistant Professor, Department of Civil Engineering, Tanta University, Tanta, Egypt.

*Corresponding author E-mail: islam_elkourashi@f-eng.tanta.edu.eg

ABSTRACT:

The main factors affecting the soil-geogrid interaction are friction, interlocking of the soil through the apertures and the soil particles size. In the present study a hypothesis assumption of modifying the conventional Biaxial Geogrid by adding cubic cogs distributed in a sine wave order on both sides of the geogrid ribs, that could improve the soil-geogrid interaction by generate interlocking mechanism between the ribs and the soil. "ICB-GGR" is the name of the proposed geogrid as an abbreviation for Isometric Cogged Biaxial Geogrid. To achieve the main goal of this study, an experimental test program was implemented and the conducted results were used in executing a numerical model of the laboratory tests using the PLAXIS 2D program. Results of the experimental tests showed improvement in shear resistance of about 50% when using the ICB-GGR in sand compared to using the Biaxial Geogrid under the same conditions. Typically, reliable numerical model has been established and achieved compliance with the experimental results by about 88%.

KEYWORDS: Biaxial Geogrids, Crushed Lime Stone, Cogged Geogrid, Numerical Analysis, Pull-out Test, , Sandy Soil, Shear Resistance.

دراسة معملية ورقمية للشبكات المسننة المصنعة ثنائية المحور

إسلام أنس القرشي^{*} و محمود أبو بكر الصديق¹ و عبد الراضي حسن¹ و يسري موافي¹ و أحمد فاروق²
¹ قسم الهندسة المدنية، كلية الهندسة، جامعة الأزهر، القاهرة، مصر.
² قسم الهندسة الإنشائية، كلية الهندسة، جامعة طنطا، طنطا، مصر.

* البريد الإلكتروني للباحث الرئيسي: islam_elkourashi@f-eng.tanta.edu.eg

الملخص:

إن العوامل الرئيسية المؤثرة على التفاعل بين التربة والشبكات المصنعة هي: الاحتكاك والتداخل بين حبيبات التربة من خلال فتحات الشبكات المصنعة بالإضافة لحجم حبيبات التربة. في هذه الدراسة تم افتراض نظرية بأن تعديل الشكل التقليدي للشبكات المصنعة بإضافة سنون مكعبة موزعة بشكل زاوية الجيب على جانبي أضلاع الشبكة يمكن أن يحسن التفاعل بين الشبكة والتربة عن طريق توليد آلية تداخل بين الأضلاع والتربة. تم تقديم الشبكة المبتكرة باسم " الشبكة المسننة المصنعة ثنائية المحور". ولتحقيق الهدف الرئيسي من الدراسة، نُفذت تجارب معملية واستخدمت النتائج المستخلصة لتنفيذ نموذج رقمي للاختبار المعمل باستخدام برنامج ثنائي الإبعاد. وقد أظهرت نتائج الاختبارات المعملية تحسناً في مقاومة القص يقدر ب 50% عند استخدام الشبكة المسننة في الرمل مقارنة بنتائج اختبارات الشبكة التجارية

تحت نفس الظروف. وعلى نحوٍ عالٍ من التطابق، بينت نتائج التحليل الرقمي توافقاً بنسبة حوالي ٨٨% مع نتائج الاختبارات المعملية.

الكلمات المفتاحية: الشبكات المصنعة ثنائية المحور، كسر الحجر الجيري، الشبكات المسننة المصنعة ثنائية المحور، التحليل الرقمي، اختبار الشد، التربة الرملية، مقاومة القص.

1. INTRODUCTION

A conference in 1984 was helpful in bringing geogrids, which were invented by Dr. Brian Mercer (Blackburn, UK), to the engineering design community. The development by Dr. Mercer led to the uniaxial (single direction stretch) geogrid with rectangular apertures and the biaxial (two directions stretch) geogrid with virtually square apertures, while the latest development in stiff polymer geogrid was released by Tensar Company, branded (TriAx 2007), a product with triangular apertures.

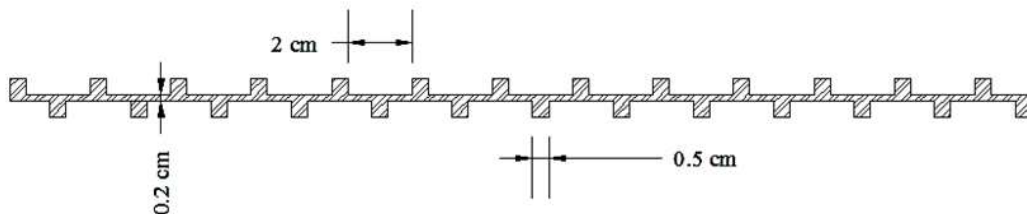
For geogrids to function properly as reinforcement, it is the interlocking of the soil through the apertures of the geogrid that achieves an efficient interlocking effect. Pinto (2004) explaining why the interlocking effect is negligible when the soil particles are small as there is no passive strength developed against the geogrid.

In order to exclude that exception, a hypothesis was assumed that reforming the conventional shape of the Biaxial Geogrid by adding cubic cogs distributed in a sine wave order on both sides of the ribs could improve the soil-geogrid interaction by generating interlocking mechanism between the ribs and the soil in addition to the existing mechanism between the soil particles through the apertures.

To ensure aforementioned hypothesis, a prototype was designed to be basically a biaxial geogrid with the aperture shape of identical square, then cubic cogs were added to the design in a sine wave order on both sides of the ribs, as shown in Figure (1). The proposed design was denominated "ICB-GGR" as an abbreviation for Isometric Cogged Biaxial Geogrid.



a)



b)

Figure (1) a) A photo for the ICB-GGR; b) Full detailed side view section showing the distribution of cogs on both sides of the ribs.

Depending on the early trials done by Vidal in order to make a testable prototype, as the polymeric production faced many manufacturing problems, steel prototypes were used for both of the ICB-GGR and the commercial Biaxial Geogrid. In order to verify the reliability of the design, steel prototypes of ICB-GGR, Biaxial Geogrid and Solid Plate were compelled to

experimental program that was implemented according to the previous work of Senoon and Farghal (2003), Duszynska and Bolt (2004), Koerner (2005), Abdel-Rahman et al. (2007), Hsieh et al. (2011), Moraci and Cardile (2012), and Mosallanezhad et al. (2016).

Thereafter, the conducted results were used to simulate some hypothetically cases of Mechanically Stabilized Earth (MSE) using a finite element analyzing program PLAXIS 2D in the light of researches of Hussein et al. (2009),Mahmood (2009), Husseinand Meguid (2013).

2. EXPERIMENTAL PROGRAM

Pull-out tests were operated according to ASTM D 6706-0101 with some modifications to suit the laboratory preparations. Besides the manufacturing obstacles of polymeric prototype of the ICB-GGR, steel 37 was the most appropriate material to accomplish the research since the main target is to investigate the shape effect of the proposed ICB-GGR.

2.1 TESTING MATERIALS

In order to study the improvement in the soil-cogged geogrid interaction, three prototypes, with the same dimensions of apertures, were manufactured of steel 37. As shown in Figure (2), the first prototype is a solid plate representing the concept of reinforcing soil, the second is the conventional Biaxial geogrid and the last one is the proposed ICB-GGR. Prototypes of the Solid Plate and the Biaxial Geogrid were formed from a solid steel sheetby using means of lasercutting. On the other hand,TIG welding technique was used to assemble laser cut ribs to form the shape of the ICB_GGR, which was described previously by Anas et al. (2016).

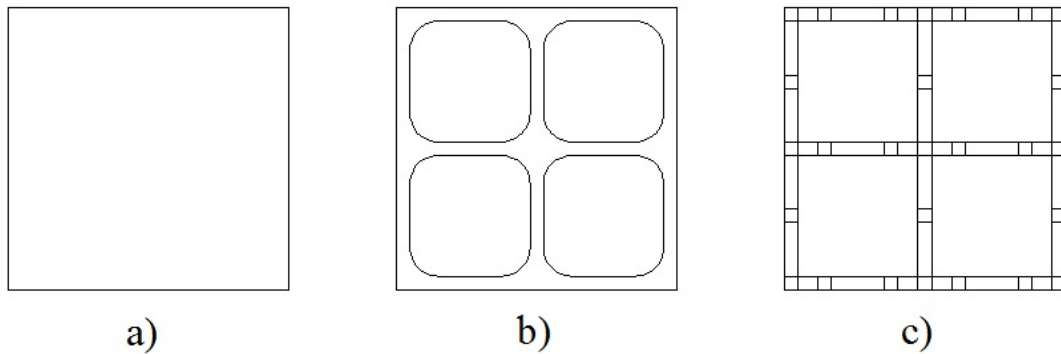


Figure (2) The tested prototypes, a) Solid Plate; b) Biaxial Geogrid; c) ICB-GGR.

The three prototypes dimensions are concluded in Table (1).

Table (1) Dimensions of the three prototypes used in the experimental study.

Prototype	Length (mm)	Width (mm)	Height (mm)	Apertures (mm)
Solid Plate	1000	600	2	-
Biaxial Geogrid	1000	600	2	50*50
ICB-GGR	1000	600	2 (ribs)	50*50
Cubic Cogs	5	5	5	20 (between cogs)

The reinforcement prototypes were used to reinforce uniformly graded sand in its loose case and crushed lime stone. Table 2 shows the characteristics of both types of soil.

Table (2) The characteristics of types of soil used in the experimental study.

Soil	Sand	Crushed Lime Stone
Dry Density	16 kN/m ³	14 kN/m ³
Internal Friction Angle Φ	28°	42°
D ₁₀	0.27 mm	5.2 mm
D ₆₀	0.72 mm	8 mm
Uniformity Coefficient (C _u)	2.6	1.54
Soil Grading Distribution	uniformly graded	Size No. 1

2.2 TESTMODEL

Pull-out tests were carried out according to ASTM D 6706-0101 with some modifications to suit the laboratory preparations. As shown in Figure (3), the test model consists mainly of a pull-out testing box, a steel frame mounted over the pull-out box to give the required reaction,

and a steel frame fixing the pull-out loading system mounted in front of the pull-out box. Table (3) illustrates the dimensions of the described apparatus.

Table (3) Dimensions of the test apparatus parts.

	Length (cm)	Width (cm)	Height (cm)
Steel Box	100	70	70
Reaction Frame	20	83	177
Loading Frame	10	70	82

The vertical stress was manually applied by a hydraulic jack with a maximum capacity of 1000 kN and is placed on a steel plate. The overburden pressure was uniformly distributed on the soil by means of a steel plate that has dimensions of 73 cm (length) \times 49 cm (width) \times 4 cm (depth). A manually controlled hydraulic jack having a maximum capacity of 230 kN was used for applying the pull out load.

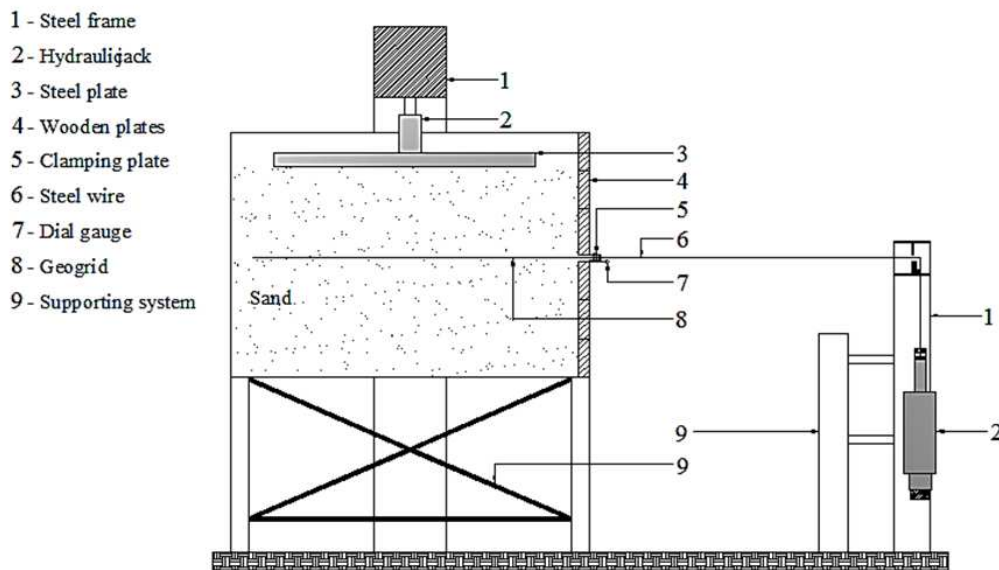


Figure (3) A schematic diagram of the pull-out testing model.

2.3 TEST PROCEDURE

In all cases of loading, the soil was prepared inside the testing box by manually pouring, and was placed in 6 layers with 10 cm thickness of each layer. A plastic can was put in the middle of each layer to ease calculating the layer density after each test. When the soil reached 30 cm of height, the reinforcement was fixed to the clamping plate and was placed over the surface of the soil. Thereafter, the rest height of the soil was completed also in three layers. Dial gauges were placed tangent to the clamping plate to measure the front displacements. The external surcharge was applied and kept constant using a hydraulic jack placed over a steel plate resting on the soil. After that, the pull-out load was kept constant between each two successive increments either for 5 minutes or till the gauges settled, whichever was longer. The pull-out load was applied using a manually controlled hydraulic jack fixed by an assembling bracing system permitting the loading wire to path through an opening in the consisting steel beam. Padding the beam with Teflon glued by epoxy was a priority to prevent the friction between the wire and the beam during the tests. According to the Egyptian Code of practice, tests failure was considered when the front displacement reach 5% of the total length of the specimen or distinctive leap of the front displacement readings occurred.

2.4 TESTS RESULTS

The results obtained from the pull-out tests are summarized next in Tables (4) and (5). In these tables, the letter (q) denotes the external surcharge, (σ_n) denotes the normal stress acting on the geogrid, (P) denotes the pull-out load measured in the test, (Q) is the pull-out resistance, (τ_{ult}) is

the interface shear strength, and (Avg. γ) is the average density of all layers measured after installing the prototypes. Noting that an extra test was implemented on the ICB-GGR due to the rupture failure of the welded joints occurred in another test.

The total normal stress σ_n (kN/m²) acting on the reinforcements was calculated using the following equation:

$$\sigma_n = \gamma h + q \dots\dots(1)$$

Where: γ (kN/m³) is the soil dry density, h (m) is the height of soil above the reinforcement, and q (kN/m²) is the applied external surcharge.

The interface shear strength (τ_{ult}) can be defined as:

$$\tau_{ult} = p/2A \dots\dots(2)$$

Where τ_{ult} (kN/m²) is the interface shear resistance, P (kN) is the pull-out load and A (m²) is the reinforcement surface area.

The friction angle of the soil-geogrid interface δ (°) is calculated as follows:

$$\tan \delta = \tau_{ult} / \sigma_n \dots\dots(3)$$

The pull-out resistance (Q) of geogrid can be calculated as follows:

$$Q = P n_g / N_g / N_g \dots\dots(4)$$

Where Q (kN/m) is the pull-out resistance, n_g is the number of ribs per unit width of the geogrid in the direction of the pull-out load, and N_g is the total number of ribs of geogrid in the direction of the pull-out load.

The friction factor characterizing the soil-geogrid interaction (α) is determined as follows:

$$\alpha = \tan \delta / \tan \phi \dots\dots(5)$$

Where ϕ (°) is the angle of internal friction of the soil.

Table (4) Summary of results of the Pull-out Tests carried out on Sand.

q kN/m ²	σ_n kN/m ²	Type of Ref.	Symbol	P (kN)	Max. Disp. (mm)	Q (kN/m)	Avg. $\gamma_{resulted}$	τ_{ult} (kN/m ²)	Mode of failure
(1)	(2)	(3)		(4)	(5)	(6)	(7)	(8)	(9)
18.8	25.16	ICB-GGR		66.02	38.01	106.65	16.54	55.02	slippage
27.25	33.61	Solid Plate		19.62	22.345	32.7	16.72	16.35	slippage
		Biaxial Geogrid		58.86	26.11	95.08	16.82	49.05	slippage
		ICB-GGR		90.74	23.6	146.58	16.96	75.62	arching
54.5	60.86	Solid Plate		22.1	20.975	36.83	16.76	18.42	slippage
		Biaxial Geogrid		93.195	24.11	150.55	16.87	77.66	slippage
		ICB-GGR		142.245	25.56	229.78	16.77	118.54	slippage
81.75	88.11	Solid Plate		47.088	16.32	78.48	16.77	39.24	slippage
		Biaxial Geogrid		110.36	20.145	178.27	16.97	91.97	slippage
		ICB-GGR		125.08	13.93	202.05	16.87	104.23	rupture

Table (5) Summary of results of the Pull-out Tests carried out on Crushed Lime Stone.

q kN/m ² (1)	σ_n kN/m ² (2)	Type of Ref. (3)	Symbol (4)	P (kN) (4)	Max. Disp. (mm) (5)	Q (kN/ m) (6)	Avg. $\gamma_{resulted}$ (7)	τ_{ult} kN/m ² (8)	Mode of failure (9)
9	13.18	Solid Plate		14.715	20.84	23.77	14.4	12.26	slippage
		Biaxial Geogrid		87.31	14.26	141.04	14.97	72.76	arching
		ICB-GGR		88.29	16.185	142.62	14.87	73.58	arching
9.81	14	Solid Plate		18.64	20.29	30.11	14.77	15.54	slippage
		Biaxial Geogrid		88.29	15.1	142.62	14.62	73.58	arching
		ICB-GGR		98.1	13.06	158.47	14.85	81.75	arching
10.63	14.81	Solid Plate		19.62	23.645	31.7	14.76	16.35	slippage
		Biaxial Geogrid		93.2	13.39	150.55	15.11	77.67	arching
		ICB-GGR		116.74	17.785	188.58	15	97.28	arching

It is to be noted that, as resistance of the crushed lime stone was higher than the sand under the same circumstances. Therefore the three values of overburden pressures (q) were reduced when using the crushed lime stone to the values of 8.45 kN/m², 9.27 kN/m², and 10.1 kN/m². In Figure (4) when using sand soil, it can be seen that as the normal pressure acting on the tested soil reinforcements increases, the maximum front displacements before failure decrease. The maximum front displacement values, in case of the Solid Plate, were higher than those for the Biaxial Geogrid and the ICB-GGR at the whole range of the applied normal stress, as shown in Figure (5). Figure (6) illustrated that, for the three types of reinforcement, density of the reinforced soils increased at the end of the tests. However, the percentage of density increasing differentiates from reinforcement to another under the same circumstances. As shown in Figure (7), for the three prototypes, the interface shear strength increases with the increasing of the normal stress. The interface shear strength in case of using the ICB-GGR is higher than that in case of using the Biaxial Geogrid by about 50%. In the case of Crushed lime stone, the values of shear resistance with the ICB-GGR and the Biaxial geogrid have nearly close values, although the improvement in values of shear resistance started to appear with the increasing of normal stress, as shown in Figure (8).

When calculating the friction angle of a soil-reinforcement interface δ , the highest value was recorded in case of using the ICB-GGR and it is nearly 64.76°, then came the Biaxial Geogrid with $\delta = 51.24^\circ$. The lowest value was recorded when using the Solid Plate with a value of 22.27°. The obtained calculated values of the friction factor are $\alpha_{Solid\ Plate} = 0.77$, $\alpha_{Biaxial\ Geogrid} = 2.35$, and $\alpha_{ICB-GGR} = 4$.

In the case of crushed lime, the values of the friction angle of a soil-reinforcement when using the ICB-GGR with $\delta = 81.34^\circ$, then the Biaxial Geogrid with $\delta = 79.2^\circ$. The lowest value was recorded when using the Solid Plate with $\delta = 47.83^\circ$. The obtained calculated values of friction factors are $\alpha_{Solid\ Plate} = 1.27$, $\alpha_{Biaxial\ Geogrid} = 6.03$, and $\alpha_{ICB-GGR} = 7.56$. The values of friction factor exceeding 1 were presented in previous researches by Mosallanezhad et al. (2016) and Makkaret al.(2017).

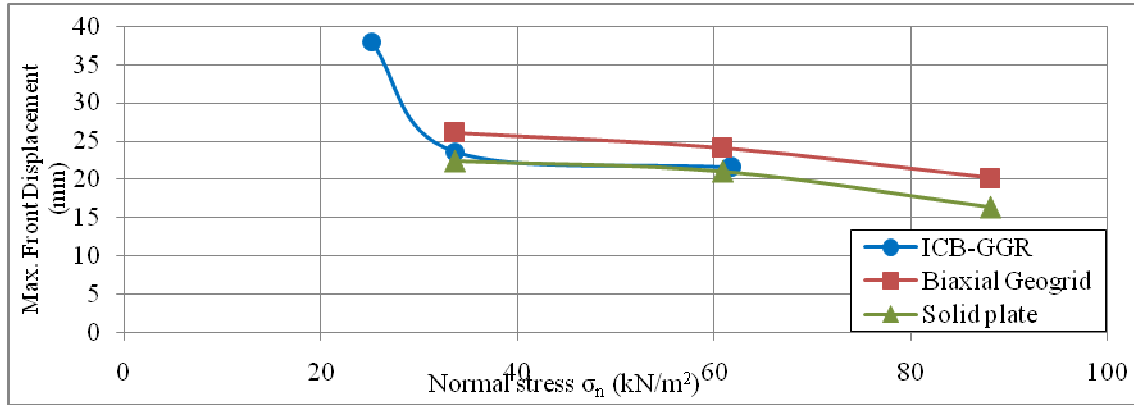


Figure (4) Effect of applying different values of normal stress on the max. front displacement of soil reinforcements embedded in sand.

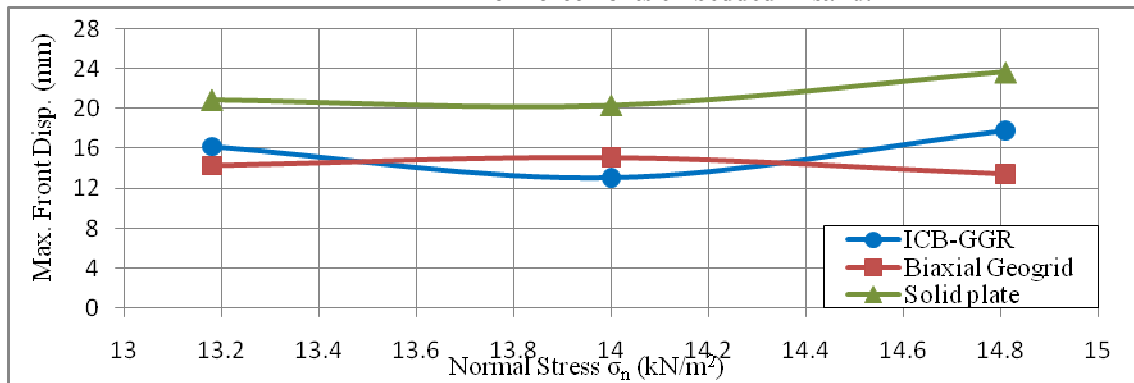


Figure (5) Effect of applying different values of normal stress on the max. front displacement of different reinforcements embedded in crushed lime stone.

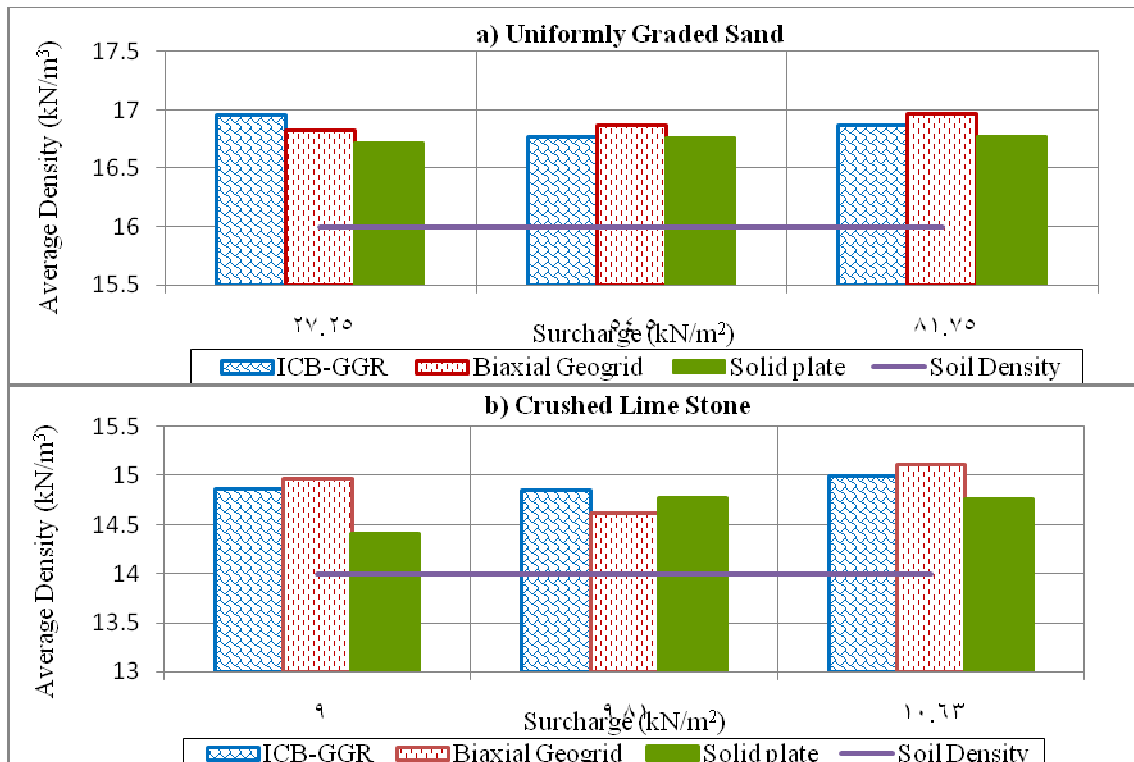


Figure (6) Average densifying values caused the three grids reinforcing soil.

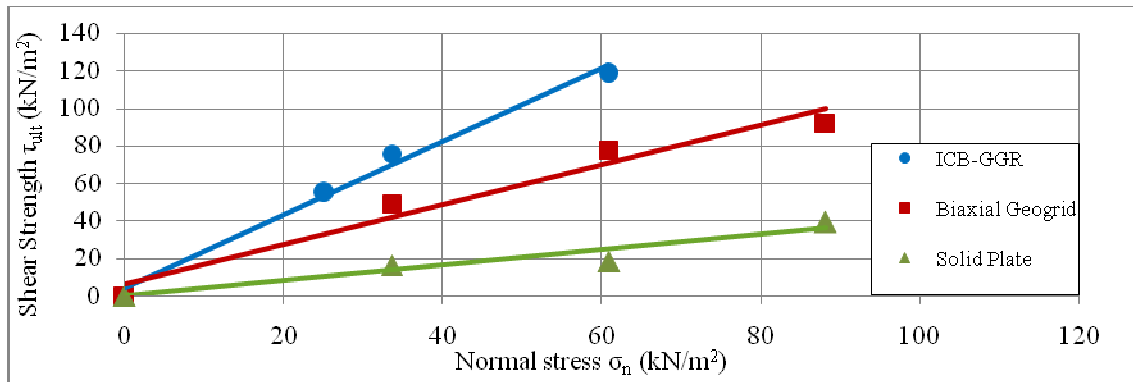


Figure (7) Effect of using different types of reinforcement on the shear strength of sand.

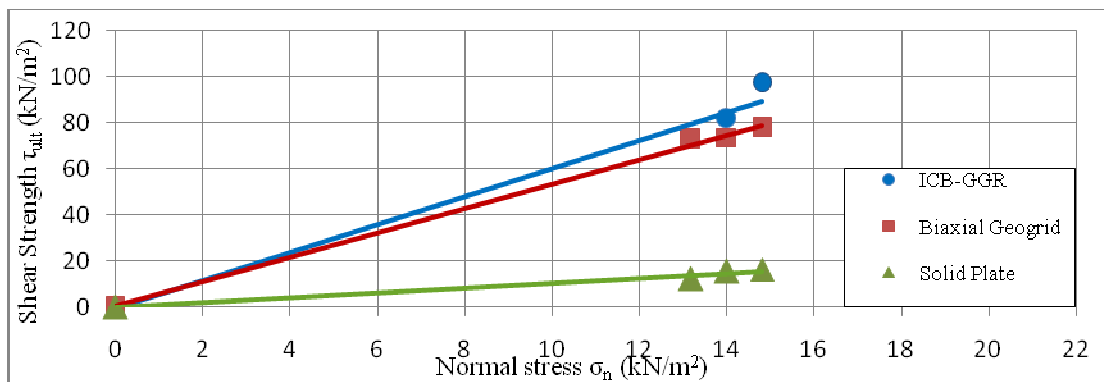


Figure (8) Effect of using different types of reinforcement on the shear strength of crushed lime stone.

3. NUMERICAL STUDY

The results prescribed by Elkorashi (2017), clarified that the pull-out resistance of the proposed ICB-GGR in sand superior the conventional Biaxial Geogrid, in sand, by about 50%, while the percentage of improvement was about 25% in the case of reinforcing crushed lime stone. The numerical simulation depended on the extracted data from pull-out tests in sand.

Soil has nonlinear elastoplasticbehaviourand “PLAXIS 2D” program was used to simulate the laboratory pull-out tests.

3.1 MODELLING ASPECTS

The Plaxis program can handle cohesionless sand ($c = 0$), but some options will not perform well. To avoid complications, non-experienced users are advised to enter at least a small value (use $c > 0.2$ kPa) (PLAXIS, 2002). The interface properties are calculated from the soil properties in the associated data set and the strength reduction factor by applying the following rules:

$$c_i = R_{inter} c_{soil} \dots\dots(2)$$

where: c_i is the interface friction factor with soil, R_{inter} is the strength reduction factor, c_{soil} is the soil cohesion factor.

The modeling properties of the steel Solid Plate, steel geogrids, and soil are listed in Tables (6), (7), and (8) respectively. The values of k_x , k_y , E_{ref} and ν were chosen to be compatible with test materials.

Table (6) Modelling parameters for the Solid Plate.

Unit	Value	Name	Parameter
kN/m	400000	EA	Axial stiffness per unit strain
kN/m ² /m	0.133	EI	Bending stiffness
m	0.002	d	Thickness of plate
kN/m/m	0.156	W	Weight of plate
-	0.25	v	Poisson's Ratio

Table (7) Modelling parameters for geogrid.

Unit	ICB-GGR	Biaxial Geogrid	Name	Parameter
kN/m	84000	42000	EA	Axial stiffness per unit strain
kN/m	230	178	N _p	Maximum axial force per unit length

Table (8) Material properties of the sand and interface element.

Unit	Interface	Sand	Name	Parameter
-	Mohr-Coulomb	Mohr-Coulomb	Model	Material model
-	Drained	Drained	Type	Type of material behaviour
kN/m ³	16	16	γ _{dry}	Dry soil weight
kN/m ³	17.46	17.46	γ _{wet}	Wet soil weight
m/day	1.0	1.0	k _x	Permeability in h _{a1} direction
m/day	1.0	1.0	k _y	Permeability in v _{a1} direction
kN/m ²	13000	13000	E _{ref}	Young's modulus (constant)
-	0.3	0.3	v	Poisson's ratio
kN/m ²	variable	variable	c _{ref}	Cohesion (constant)
◦	variable	28	Φ	Friction angle
◦	variable	0.0	ψ	Dilatancy angle

The model of the pull-out laboratory test is illustrated in Figure (9).

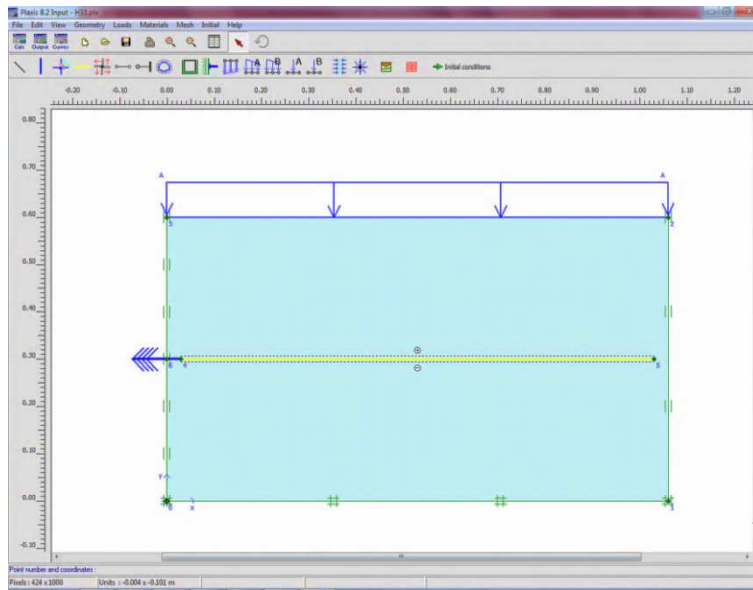


Figure (9) Numerical model of the pull-out test.

Table (9) Comparison between PLAXIS and lab.results.

Error (%)	Q Lab. results (kN/m)	Q Plaxis results (kN/m)	Symbol	Type of RFT	q (kN/m ²)
7.82	106.65	114.99		ICB-GGR	18.8
3.49	32.7	31.56		Solid Plate	27.25
5.4	95.08	100.22		Biaxial Geogrid	
10.11	146.58	131.75		ICB-GGR	54.5
27.95	36.83	51.12		Solid Plate	
14.31	150.55	129		Biaxial Geogrid	
23.52	229.78	175.73		ICB-GGR	81.75
9.9	78.48	70.71		Solid Plate	
16.4	178.27	149.04		Biaxial Geogrid	
4.44	202.05	206.49		ICB-GGR	

Figure (10) shows the results of deformed mesh, and the results of all simulations are tabulated in Table (9) and plotted in Fig. (11).

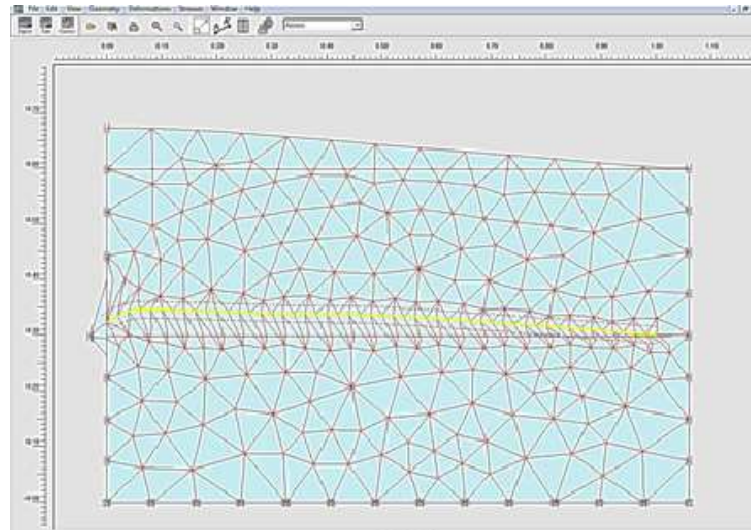


Figure (10) Deformed mesh for pull-out test.

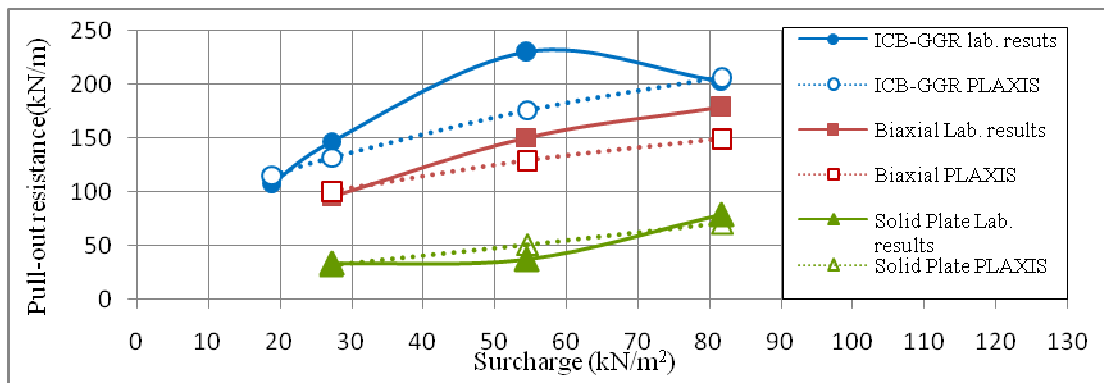


Figure (11) Pull-out resistance due to laboratory and PLAXIS results.

4. CONCLUSION

The main conclusions drawn from the pull-out tests and finite element simulation with “*PLAXIS*” can be summarized as follows:

1. Values of the pull-out resistance, the shear resistance and the pull-out capacity obtained in case of reinforcing the tested sand with the new proposed ICB-GGR are about 50% higher than these obtained when using the conventional Biaxial Geogrid and are about 453% higher than these obtained when using the Solid Plate.
2. The friction angle between the proposed ICB-GGR and the sand is higher than that between the sand and the Solid Plate by about 42.49°, and is higher than that between the conventional Biaxial Geogrid by about 13.52°.
3. The friction factor α achieved in case of using the proposed ICB-GGR is nearly 70% over the factor obtained when using the Biaxial Geogrid and is about 419% over the factor obtained when using the Solid Plate.
4. The pull-out resistance, the shear resistance, the pull-out capacity and the friction factor α obtained in case of reinforcing crushed lime stone with the new proposed ICB-GGR are about 25 % higher than those obtained when using the conventional Biaxial Geogrid and are about 495% higher than those obtained when using the Solid Plate.
5. The friction angle of a soil-reinforcement interface in the case of using the proposed ICB-GGR is higher than the angle obtained in case of using the Solid Plate by about 33.51°, and superior the case of using the conventional Biaxial Geogrid by about 2.23°.
6. Simulation of the pull-out tests for the proposed ICB-GGR, the conventional Biaxial Geogrid and the Solid Plate reinforcing sand are highly in agreement with the gained results of the laboratory pull-out tests.

REFERENCES

1. Abdel-Rahman, A.H., Ibrahim, M.A.M. and Ashmawy A.K. (2007). Utilization of a large-scale testing apparatus in investigating and formulating the soil/geogrid interface characteristics in reinforced soils. *AJBAS*, 1(4), 415-430.
2. Anas, I., Farouk A., El Sideek M.B., Hassan A.R. and Mowafy Y. (2016). An Innovative Shape of Geogrid to increase Pull-Out Capacity. *IOSR-JMCE*, 13(4), 72-79.
3. Elkorashi, I. A. "Analysis of Earth Structures Reinforced by Different Geogrids Sections and Filled with Different Backfill Materials.", Master's thesis, Al-Azhar University, Cairo, Egypt, (2017).
4. Duszynska, A. and Bolt, A.F. (2004). Pullout tests of geogrids embedded in non-cohesive soil. *Hydro-Engineering and Environmental Mechanics*, 51(2), 135–147.
5. Hsieh, C.W., Chen, G.H. and Wu, J.H. (2011). The shear behavior obtained from the direct shear and pull-out tests for different poor graded soil-geosynthetic systems. *Journal of GeoEngineering*, 6(1), 15-26.
6. Hussein, M.G., Meguid, M.A., and Mowafy, Y. (2009). "On the 3D modeling of soil-geogrid interaction." Conference: GeoHalifax, the 62nd Canadian Geotechnical Conference, At Halifax, Nova Scotia, Canada, vol. 1, No. 138, pp. 986-991.
7. Hussein, M. G., and Meguid, M. A. (2013), "Three-Dimensional Finite Element Analysis of Soil-Geogrid Interaction under Pull-out Loading Condition", proceedings of the 66th Canadian Geotechnical Conference, Montreal, Quebec, Canada, September.
8. Koerner, R.M. (2005). *Designing with geosynthetics*. New Jersey: Pearson Prentice Hall.
9. Mahmood, T. "Failure analysis of a mechanically stabilized earth (MSE) wall using finite element program PLAXIS." Master Dissertation, Civil Engineering Department, University of Texas at Arlington Texas, USA, 2009.
10. Makkar, F. M., Chandrakaran, S., and Sankar, N. (2017), "Performance of 3-D geogrid-reinforced sand under direct shear mode", *International Journal of Geotechnical Engineering*, 13(3), 227-235.
11. Moraci, N. and Cardile, G. (2012). Deformative behaviour of different geogrids embedded in a granular soil under monotonic and cyclic pull-out loads. *Geotextiles and Geomembranes*, 32(3), 104-110.
12. Mosallanezhad, M., Taghavi, S.H.S., Hataf, N. and Alfaro, M.C. (2016). Experimental and numerical studies of the performance of the new reinforcement system under pull-out conditions. *Geotextiles and Geomembranes*, 44, 70-80.
13. Ottosen, N.S. and Petersson, H. (1992). *Introduction to the finite element method*. New York: Prentice Hall.
14. Pinto, M.I.M. (2003). Discussion of applications of geosynthetics for soil reinforcement. *Ground Improvement*, 7(2), 61–72.
15. PLAXIS (2002). *Finite Element Code for Soil and Rock Analysis*. Rotterdam: A. A. Balkema publishers.
16. Senoon, A-A.A. and Farghal, O.A. "Influence of the confinement, soil density, and anchorage length of reinforcement on soil geogrid interaction." In Proceedings of Conference of Civil Engineering Science, Assiut University, Assiut, 2003, pp. 232-241.